Applied Surface Science 257 (2011) 5460–5464

Contents lists available at ScienceDirect

Applied Surface Science

journal homepage: www.elsevier.com/locate/apsusc

# Recent developments in the formation and structure of tin–iron oxides by laser pyrolysis

R. Alexandrescu[a,*], I. Morjan[a], F. Dumitrache[a], R. Birjega[a], C. Fleaca[a], I. Soare[a], L. Gavrila[a], C. Luculescu[a], G. Prodan[b], V. Kuncser[c], G. Filoti[c]

[a] National Institute for Lasers, Plasma and Radiation Physics, POB MG-36, Bucharest 077125, Magurele, Romania
[b] Ovidius University of Constanta, Bd. Mamaia 124, Constanta, Romania
[c] National Institute of Materials Physics, POB MG-7, Bucharest 077125, Magurele, Romania

ARTICLE INFO

*Article history:*
Received 26 May 2010
Received in revised form 1 October 2010
Accepted 18 November 2010
Available online 26 November 2010

*Keywords:*
Tin oxide
Nanoparticles
Laser pyrolysis
Fe doped $SnO_2$
Tin–iron oxides
Mössbauer spectroscopy

ABSTRACT

Complex oxides demonstrate specific electric and magnetic properties which make them suitable for a wide variety of applications, including dilute magnetic semiconductors for spin electronics. A tin–iron oxide $Sn_{1-x}Fe_xO_2$ nanoparticulate material has been successfully synthesized by using the laser pyrolysis of tetramethyl tin–iron pentacarbonyl–air mixtures. Fe doping of $SnO_2$ nanoparticles has been varied systematically in the 3–10 at% range. As determined by EDAX, the Fe/Sn ratio (in at%) in powders varied between 0.14 and 0.64. XRD studies of $Sn_{1-x}Fe_xO_2$ nanoscale powders, revealed only structurally modified $SnO_2$ due to the incorporation of Fe into the lattice mainly by substitutional changes. The substitution of $Fe^{3+}$ in the $Sn^{4+}$ positions ($Fe^{3+}$ has smaller ionic radius as compared to the ionic radius of 0.69 Å for $Sn^{4+}$) with the formation of a mixed oxide $Sn_{1-x}Fe_xO_2$ is suggested. A lattice contraction consistent with the determined Fe/Sn atomic ratios was observed. The nanoparticle size decreases with the Fe doping (about 7 nm for the highest Fe content). Temperature dependent $^{57}$Fe Mössbauer spectroscopy data point to the additional presence of defected $Fe^{3+}$-based oxide nanoclusters with blocking temperatures below 60 K. A new Fe phase presenting magnetic order at substantially higher temperatures was evidenced and assigned to a new type of magnetism relating to the dispersed Fe ions into the $SnO_2$ matrix.

## 1. Introduction

$SnO_2$ with a wide band gap of 3.6 eV is a photoactive material [1] and a potentially attractive semiconductor host matrix for introducing transition metal ions. Structural modifications of $SnO_2$ due to the incorporation of the Fe into the lattice refer mainly to substitutional changes and are the subject of recent debates on the magnetism of Fe-doped $SnO_2$ ferromagnetic semiconductors [2], as a second generation of spin electronics. Structural changes associated with the doping are dependent on the synthesis method. This statement is particularly true in case of the bottom-up approaches (such as aerosols methods [3]) where process control over particle size dimensions applies.

The laser pyrolysis bases on the overlapping of the emission line of the $CO_2$ laser with an absorption line of one or more precursors [4]. This method has many advantages over chemical/solution synthesis methods. It is a single step-method, which provides high purity products since the reaction takes place far from the reactor walls. Nucleated particles are dry and collected directly on the filter and in the collection chamber. Due to both the milliseconds time scale in which particles are formed and the high heating/cooling rates evolving near the reaction zone (well defined by the focused laser spot), the freshly nucleated particles are rapidly quenched to low mean diameters (typically below 10 nm in case of iron compounds) and narrow size distributions.

In our previous studies [5] we have reported on the single-step synthesis of $SnO_2$-based nanoparticles using the pyrolysis of tetramethyl tin (TMT) sensitized with ethylene mixtures. By introducing iron pentacarbonyl in the reactive mixture, simultaneous iron doping occurred. Controlled Fe/Sn atomic ratios, ranging from nominal 0 to 0.08 were used in order to prepare Fe-doped $SnO_2$-based nanopowders (at low Fe concentrations).

The main objective of this work is the development of the laser synthesis for the preparation of tin–iron oxide $Sn_{1-x}Fe_xO_2$ nanoparticulate material at higher Fe doping levels. Fe/Sn ratio (in at%) in powders has been varied between 0.14 and 0.64. The effect of the increasing presence of iron on the structure, the phase formation,

---

* Corresponding author at: National Institute for Lasers, Plasma and Radiation Physics, Laboratory of Laser Photochemistry, 111 Atomistilor St., POB MG-36, Bucharest 077125, Magurele, Romania. Tel.: +40 21 4574489; fax: +40 21 4574243.
*E-mail addresses:* ralexandrescu2001@yahoo.co.uk, rodica.alexandrescu@inflpr.ro (R. Alexandrescu).

0169-4332/$ – see front matter © 2010 Elsevier B.V. All rights reserved.
doi:10.1016/j.apsusc.2010.11.114

**Table 1**
Experimental parameters for the synthesis of $Sn_{(1-x)}Fe_xO_2$ by laser pyrolysis.

| Sample | $\Phi_{C_2H_4/Fe(CO)_5}$ (sccm) | $\Phi_{C_2H_4/Sn(CH_3)_4}$ (sccm) | $T_{flame}$ (°C) | EDAX (at%) | | | | |
|---|---|---|---|---|---|---|---|---|
| | | | | C | O | Sn | Fe | Fe/Sn |
| E06 | 0 | 30 | 615 | 12.46 | 55.65 | 31.90 | 0 | 0 |
| E9 | 10 | 20 | 617 | 12.11 | 56.88 | 27.08 | 3.93 | 0.14 |
| E10 | 17 | 13 | 630 | 14.46 | 57.91 | 21.39 | 6.24 | 0.29 |
| E8 | 15 | 15 | 630 | 14.53 | 56.01 | 21.20 | 8.26 | 0.39 |
| E7 | 20 | 10 | 650 | 17.46 | 55.56 | 16.44 | 10.54 | 0.64 |

$\Phi_{air}$ = 110 sccm, $P_{laser}$ = 85 W, $\Phi_{Ar\text{-}conf}$ = 1500 sccm, $\Phi_{Ar\text{-}w}$ = 150 sccm, $p$ = 500 mbar.

the crystallinity, the average particle diameters and the size distributions are systematically investigated. Temperature dependent $^{57}$Fe Mössbauer spectroscopy data point to the additional presence of defected $Fe^{3+}$-based oxide nanoclusters. The new Fe phase presenting magnetic order at substantially higher temperatures was assigned to a new type of magnetism, which relates to the dispersed Fe ions into the $SnO_2$ matrix.

## 2. Experimental

The synthesis of $Sn_{1-x}Fe_xO_2$ nanopowders was performed by employing a modified version of the pyrolysis set-up [6] in which $Sn(CH_3)_4$, $Fe(CO)_5$ and air, as gas phase precursors are simultaneously allowed to emerge into the flow reactor (employing a two-nozzle geometry) where they are orthogonally crossed by the laser beam (400 W nominal power, $\lambda$ = 10.6 μm). Since the reactants do not possess IR absorption bands at the $CO_2$ laser radiation, ethylene served as an energy transfer agent and as carrier for the TMT and Fe $(CO)_5$ vapor precursors. The flows of $Fe(CO)_5$ and $Sn(CH_3)_4$ were systematically varied in order to obtain increased Fe doping concentrations. Complementary Ar flows are employed for the confinement of reactant gases/nucleated particles towards the flow axis and for flushing the windows, respectively. By the sudden cooling/freezing outside the reaction zone, the aggregation of the hot freshly nucleated particles stops rapidly. Four representative composite $SnO_2$–Fe samples (labeled E9, E10, E8 and E7)-characterized by increasing Fe concentration are discussed. Table 1 lists the experimental parameters for the synthesis of these samples as compared to the undoped E06 sample. The first columns present the increase of the two metal precursors by the increase of their respective ethylene flows (the vapor carrier). With increased iron pentacarbonyl flow, the temperature – as observed by an optical pyrometer increases too.

The pure and Fe-doped tin oxide nanostructures were characterized by X-ray diffraction (XRD), energy dispersive analysis by X-rays (EDAX), transmission electron microscopy (TEM), high-resolution electron microscopy (HREM), selected area electron diffraction (SAED). Samples of different iron content were analyzed by temperature dependent $^{57}$Fe Mössbauer spectroscopy. The spectra were acquired with a Mössbauer driving system operating in constant acceleration mode combined with conventional electronics and a $^{57}$Co(Rh matrix) source of about 25 mCi activity.

## 3. Results and discussion

Depending on the preparation technique, the tin oxide phase composition and the dispersion of iron in the different phases may vary in the specimens. Factors such as morphology, particle surface area and the presence of defects could largely affect the iron site distribution as well as their specific magnetic interactions.

The last column of Table 1 presents the elemental content of the samples in carbon, oxygen, tin and iron – as determined by the EDAX. The Fe/Sn ratio (in at%) in powders was varied between 0.14 and 0.64 (the Fe concentration increases from about 3 at% (sample E9) to 10 at% (sample E7)).

Carbon contamination (12–17 at% C content in samples) is found in samples due to the unwanted ethylene sensitizer decomposition. This decomposition is speeded up by the increase of the reaction temperature, as shown in Table 1 (650 °C in case of sample E7, with 20 sccm ethylene carrier). We should note here the role of the freshly formed iron nanoparticles in speeding up the hydrocarbon dissociation [7]. The presence of quasi-amorphous carbon in the environmental matrix was observed in previous laser pyrolysis experiments [7,6].

X-ray diffraction analysis for the reference iron-free sample and for the samples doped with different iron concentration in the 2-theta angular range (from 20° to 90°) was performed and is displayed in Fig. 1. The structural data of the analyzed samples are gathered in Table 2. The examination of the diffractogram of the pure Sn oxide indicates a mixture of the rutile-cassiterite $SnO_2$ and the metastable romarchite SnO. With increasing Fe doping, the tin oxide nanomaterials exhibit a single $SnO_2$ structure without any indications for the formation of other crystalline by-products.

No amount of any crystalline iron compounds could be detected which could be indicative of highly dispersed iron either entered in substitutional positions or partially forming an amorphous to XRD phase. One observes increased asymmetry of XRD lines with increasing Fe in samples, probably due to a small deformation of the tin oxide matrix. Thus, the $(h\,k\,0)$ lines are larger while the $(h\,0\,l)$ and $(0\,0\,l)$ lines are narrower than the $(h\,k\,l)$ standard diffraction

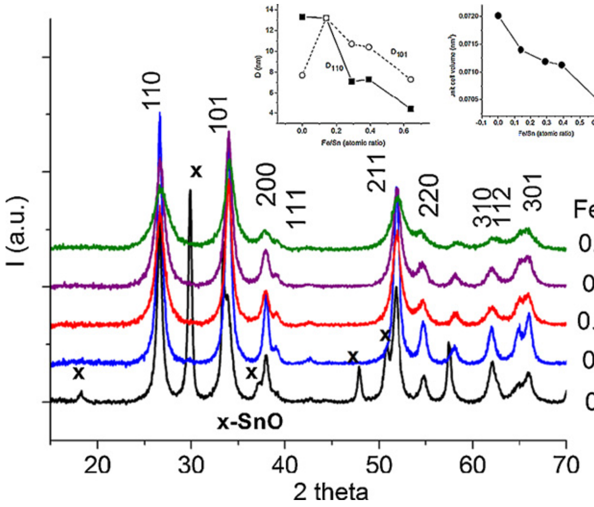

**Fig. 1.** XRD patterns for $Sn_{(1-x)}Fe_xO_2$ samples at increasing Fe/Sn ratios. The first inset presents both the anisotropy induced by the $Fe^{3+}$ substitution and the decrease of the values for the Scherrer crystallite grain size at higher doping concentration. The second inset shows the decrease of the unit cell volume with increasing Fe/Sn atomic ratios.